Body mass variability is represented by distinct functional connectivity patterns

Jennifer R Sadler[1], BA, Grace E Shearrer[1], PhD, *Kyle S Burger[1,2], PhD, MPH, RD
1. Department of Nutrition, Gillings School of Global Public Health, University of North Carolina at Chapel Hill
2. Biomedical Research Imaging Center, University of North Carolina at Chapel Hill School of Medicine

*Corresponding Author:
Kyle S. Burger
2223 McGavran Greenberg Hall
135 Dauer Drive
Chapel Hill NC 27599

Keywords: functional connectivity, twins, BMI, Default mode network, DMN, insula, obesity, dlPFC, striatum, satiation
Main Text Word Count: 5084
Abstract Word Count: 298

Abstract

Understanding weight-related differences in functional connectivity provides key insight into neurocognitive factors implicated in obesity. Here, we sampled three groups from human connectome project data: 1) 47 pairs of BMI-discordant twins (n=94; average BMI-discordancy 6.7 $\pm$ 3.1 kg/m^2), 2) 47 pairs of gender and BMI matched BMI-discordant, unrelated individuals, and 3) 47 pairs of BMI-similar twins to test for body mass dependent differences in between network functional connectivity. Across BMI discordant samples, three networks appeared to be highly sensitivity to weight status; specifically, a network compromised of gustatory processing regions, a visual processing network, and the default mode network (DMN). Further, individuals with a lower BMI relative to their twin had stronger connectivity between striatal/thalamic and prefrontal networks (*pFWE* = 0.04) in the BMI-discordant twin sample. Cortical-striatal-thalamic networks underlie regulation of hedonically motivated behaviors. Stronger connectivity may facilitate increased regulation of decision-making when presented with highly rewarding, energy-dense foods. We also observed that individuals with a higher BMI than their twin had stronger connectivity between cerebellar and insular networks (*pFWE* = 0.04). Increased cerebellar-insula connectivity is associated with caloric deprivation and, in high BMI individuals, is associated compromised satiation signaling, thereby increasing risk for postprandial food intake. Connectivity patterns observed in the BMI-discordant twin sample were not see in a BMI-similar sample, providing evidence that the results are specific to BMI discordance. Beyond the involvement of gustatory and visual networks and the DMN, little overlap in results were seen between the two BMI-discordant samples. This may be a function of the higher study design sensitivity in the BMI-discordant twin sample, relative to the more generalizable results in the unrelated sample. These findings demonstrate that distinct connectivity patterns can represent weight variability, adding to mounting evidence that implicates atypical brain functioning with the accumulation and/or maintenance of elevated weight.

Obesity is a chronic disease that affects two thirds of American adults (Flegal et al., 2012), and is associated with increased risk of metabolic disorders (Alberti et al., 2005), cardiovascular disease (Hubert et al., 1983), certain cancers (Calle and Kaaks, 2004), and mortality (Masters et al., 2013). Moreover, the prevalence of obesity is rapidly increasing worldwide (Collaborators, 2017). This is highly concerning given that the efficacy of behavioral weight loss efforts are highly variable (Dombrowski et al., 2014; Loveman et al., 2011). A myriad of internal mechanisms and external stimuli influence weight regulation, such as: physiological appetitive feedback systems, reinforcement-driven eating habits, emotional and social cues, and stimuli from the food environment (Berthoud, 2006). Additionally, behavioral constructs such as impulsivity (Nederkoorn et al., 2006), inhibitory control (Lavagnino et al., 2016), and taste sensitivity (Grinker et al., 1972) are theorized to impact weight. The brain is the key integration point for processing these factors, incorporating inputs (e.g., homeostatic satiation signaling, attentional processing) to direct food intake behaviors, thereby influencing weight (Morton et al., 2006). The examination of dynamic temporal correlations in the brain, i.e., functional connectivity, has provided considerable insight into aberrant resting-state brain networks (RSNs) associated with cognitive disease states (Van Den Heuvel and Pol, 2010; Woodward and Cascio, 2015). Therefore, a thorough understanding of how neural patterning varies with weight status is needed to accurately comprehend the neural correlates of weight regulation. Limited, but increasing evidence identify an association between elevated weight and altered neural functioning. For example, relative to healthy-weight, obesity was associated with decreased functional connectivity within networks comprising the medial prefrontal cortex and default mode network in response to viewing food stimuli (García-García et al., 2013), and with decreased functional connectivity within prefrontal and feeding circuits during taste administration of a milkshake (Geha et al., 2016). Further, obesity also was linked to increased connectivity within the attention network (premotor areas, superior parietal lobule, and visual cortex), as well as, stronger hypothalamic-striatal and amygdala-insular connectivity (Lips et al., 2014). Collectively, these data provide early indication that elevated weight is associated with disruption in the functional integration of brain regions and networks that encode aspects of hedonically motivated behaviors, gustatory, and attentional processing. Though current data are limited to smaller sample sizes, so a more detailed understanding of alterations in functional connectivity associated with elevated weight in a large sample is warranted.

Genetic composition also influences functional connectivity of RSNs (Glahn et al., 2010; Yang et al., 2016), which introduces variability in between-group investigations of weight status and RSN connectivity. Twin study designs provide a powerful approach to control for unmeasured confounds such as heritability and food environment during childhood when examining factors impacting weight status (Barsh et al., 2000; Farooqi and O'rahilly, 2000). In a small sample of female twins, increased weight was associated with decreased lateral functional connectivity within the striatum, providing evidence that brain-level effects studied with twin designs are sensitive to relatively small differences in weight (mean BMI-discordancy 3.96 kg/m^2)(Doornweerd et al., 2017). Broadly, existing investigations of weight-related RSN connectivity have compared effects between traditional BMI categories (e.g., healthy weight [BMI=18.5-24.9] vs. overweight [BMI=25.0-29.9] vs. obese [BMI>30.0]) (García-García et al., 2013; Geha et al., 2016; Lips et al., 2014). However, BMI categories are arbitrary in nature, providing little clinically relevant information when individuals are near a cut-point). Importantly, relatively small fluctuations in body weight can significantly impact health (Jensen et al., 2013). For example, decreasing weight by ~5% can improve physiological predictors of disease (Blackburn, 1995; Douketis et al., 2005). As such, weight loss interventions typically do not use transitions from one BMI category to another as a metric of success, instead focusing on within-subject weight change. A twin study design that draws on the strength of testing relative weight difference, agnostic to BMI categories, can provide a highly sensitive test of the impact of elevated weight on RSNs, while maintaining direct relevance to weight loss recommendations

and interventions. Despite these advantages, twin study designs are limited in their generalizability to the population at large (Kukull and Ganguli, 2012). However, a parallel analysis in unrelated, BMI-discordant individuals can be leveraged to test the impact of weight on RSN connectivity simultaneously providing a metric of reliability and increasing generalizability.

Here, we sought to determine weight dependent differences in functional connectivity patterning. To achieve this aim, we performed functional connectivity analyses in three independent samples: 1) a BMI-discordant twin sample; 2) a gender and BMI discordancy-matched, unrelated sample; and 3) a BMI-similar twin sample. BMI dependent connectivity patterns observed in both the BMI-discordant twin and unrelated samples allows for identification of weight dependent altered functional connectivity that is stable across two samples and is generalizable to unrelated individuals. Confirmation that these RSNs patterns are not observed in a weight-similar sample provides support that the findings are not a result of an unseen third-variable confound. Based on studies of obese versus healthy weight groups (García-García et al., 2013; Geha et al., 2016), we hypothesized that differences in BMI-discordant twins will be observed in connectivity between insular and frontal RSNs, specifically where lighter twins will show stronger connections to the insular and frontal networks.

Methods

Sample selection. All data were drawn from the HCP900-PTN data release the from the Human Connectome Project (HCP) (Van Essen et al., 2012). A visual representation of the sample selection procedures can be seen in **Figure 1**. HCP900-PTN data included 820 young adults, of which 410 individuals were twins. From the twin subsample, 98 participants were excluded from the analysis due to: incomplete data/not having a corresponding twin in the sample (n = 92), or a BMI < 18.5 (n = 6). Of the remaining 312 twin participants (n_{pairs} = 156), twin pair BMI discordancy, defined as the between twin difference in BMI (heavier twin's BMI - lighter twin's BMI), was calculated. BMI-discordant twin sample were defined using the upper tertile of BMI discordancy of the 312 twin participants. The BMI-similar twin sample was selected to have the same proportion of monozygotic and dizygotic twin pairs as the BMI-discordant sample, while maintaining a similar BMI in the twin pairs. Thus, the two twin analyses included a total sample of 188 twins (n_{pairs} = 94; 47 pairs per sample). To examine aspects of generalizability, unrelated, BMI-discordant participants (n_{pairs} = 47) were also selected from the non-twin participants included in the HCP900-PTN data. These unrelated, BMI-discordant pairs were selected to match the discordant twin sample on both BMI and gender. No significant differences between the unrelated and twin BMI-discordant samples were observed for gender, BMI, or BMI discordancy (p's > 0.95).

Data description and preprocessing. Participants completed 4 resting state functional MRI (rfMRI) runs over two days (2 runs per day) totaling 58 minutes and 12 seconds of rfMRI data per participant. Scanning details for this sample have been published previously (Van Essen et al., 2012). Briefly each rfMRI scan used an eight-factor multiband, gradient echo EPI sequence with the following parameters: TR: 720ms, TE: 33.1ms, flip angle: 52 degrees, slice thickness: 2.0mm (Van Essen et al., 2012). During the rfMRI scan, participants were instructed to look at a light crosshair on a dark background projected into their field of view.

The human connectome project preprocessed all downloaded data in the HCP900-PTN release, and no additional preprocessing was performed locally. The HCP preprocessing pipeline is extensively published elsewhere and further documented is available on their website (https://www.humanconnectome.org/study/hcp-young-adult/documentation) and therefore will only be summarized here. Data were preprocessed using the recommended minimal preprocessing pipeline (Glasser et al., 2013). Independent component analysis (ICA) and FIX (FMRIB ICA-based X-noisifer) were used to assess and remove noise per participant per run

(Salimi-Khorshidi et al., 2014; Smith et al., 2013). Individual participant data was registered using the areal-feature-based alignment and the Multimodal Surface Matching algorithm ('MSMAII') (Glasser et al., 2016; Robinson et al., 2014).

Group ICA. MELODIC's Incremental Group-PCA (MIGP) was used to generate dense connectomes of all participants' individual timeseries (Smith et al., 2014). This dense connectome was then parcellated using group-ICA to create spatial-ICA network maps at dimensionalities of 15, 25, 50, 100, 200, and 300 distinct components (Glasser et al., 2016). From the HCP documentation, each component is a continuous range of values that may contain multiple spatially separate anatomical regions. The higher the number of components per map in general means the significant area per component is smaller. Given these traits of the network maps, the 25 and 100 component network maps were selected to examine the larger and more established resting state networks (using the 25 dimensionality), as well as potentially discreet regions that may drive effects (using the 100 dimensionality) (Ray et al., 2013). Given that multiple components in a given network map may include the same anatomical region, components will be referred to as independent components (ICs) with their number and anatomical region(s) comprised within e.g., occipital pole (IC 9) relative to occipital pole (IC 3). Independent components that were considered to be noise were identified by two independent researchers. Components were flagged as noise when BOLD activity was primarily following the gyri and/or solely following the surface of brain/skull (Poldrack et al., 2011). As a result, ICs 18 and 24 were determined to be noise and were removed from consideration in the 25-component parcellation.

Individual component timeseries. Per dimensionality, individual participant timeseries were concatenated and spatially mapped to the corresponding network map described above. This created a single timeseries per component per participant. Therefore, each participant had a component timeseries made up of the 4800 time points (1200 time points over 4 runs) by the number of components (15, 25, 50, 100, 200, and 300). For this analysis, each participant had a component timeseries made up of either 4800x25 or 4800x100.

Creation of netmats. The 25 and 100 component group network maps were each regressed against the corresponding individual component timeseries using the "dual-regression stage-1" approach to create individual participant network matrices (netmats) (Filippini et al., 2009).

Heritability factor calculation. To determine the effect of heritability on connectivity of each network, a heritability score (H_b^2) was calculated for each network, based on Falconer's formula (Falconer and Mackay, 1996).

$$H_b^2 = 2(r_{mz} - r_{dz})$$

We calculated the correlation between each twin pair per component in the netmat (both 25 and 100 dimensionalities separately) and averaged the correlations in both the monozygotic and dizgotic twin groups respectively to create two average correlation matrices: monozygotic (r_{mz}) and dizygotic (r_{dz}). The difference between the r_{mz} and r_{dz} matrices was calculated and multiplied by 2. The resulting heritability matrix contained a H_b^2 value for each pairwise connection between components. Individual level netmats were then each weighted by the H_b^2 matrix to adjust for heritability effects.

Statistical analyses. FSLNets (Version 0.6, FMRIB, Oxford, UK) was used to assess BMI-dependent differences between RSN connectivity. For each sample (BMI-discordant twins, BMI-similar twins, and unrelated BMI-discordant pairs), full correlations with normalized covariances were run on the netmats described above to create a correlation matrix. A single group paired T

test was performed on the correlation matrices with the following contrasts: 1) higher BMI individual compared to lower BMI individual (higher BMI > lower BMI), and 2) lower BMI individual compared to higher BMI individual (lower BMI > higher BMI). To correct for potential false positives, non-parametric permutation testing was used through FSL's randomise tool with 10,000 permutations per twin pair (or unrelated pair) (Winkler et al., 2014). Results were considered significance at $p_{FWE} < 0.05$ (Eklund et al., 2016). Negative correlations were not included in analyses, as they are not interpretable in the present context (Murphy et al., 2009).

To account for generalizability of results and heritability confounding, connectivity results within the BMI-discordant twin sample were contrasted to that of the 1) unrelated, BMI-discordant sample as a test of generalizability; and 2) in BMI-similar twin sample as a test of heritability confounding. Significant network connectivity in both contrasts was compared between BMI-discordant twins, unrelated BMI-discordant pairs, and BMI-similar twins. Equivalent results were identified when significant connectivity of two networks was observed in both samples. Connectivity results present in the both BMI-discordant pair samples (twin and unrelated), but not seen in the BMI-similar twin pairs were considered reliable and generalizable body mass contingent alterations in functional connectivity.

Secondary analyses included examination of within pair and between group differences in behavioral, mood, substance abuse, and physiological characteristics theorized to relate to eating behavior and weight regulation or that may represent unique physiological differences between BMI discordant groups not encompassed by BMI alone: response inhibition and executive functioning as measured by the NIH Toolbox's Flanker Task (age adjusted) (Lavagnino et al., 2016; Weintraub et al., 2013), self-regulation and impulsivity as measured by the Delay Discounting Task (Green et al., 1994; Nederkoorn et al., 2007), taste sensitivity as measured by the NIH Toolbox's Taste Intensity Test (age adjusted) (Coldwell et al., 2013; Grinker et al., 1972), major depressive episodes, number depressive symptoms, alcohol use, tobacco use, illicit drug use or marijuana use and dependence, hemoglobin A1c and systolic and diastolic blood pressure. Mixed linear models were used to test for within-pair and between-group differences in the behavioral and physiological measures via PROC MIXED in SAS (Version 9.4, SAS Institute Inc., Cary, NC, USA). Significance was thresholded at $p < 0.05$.

Preregistration and analytic scripts for this study can be found via the Open Science Framework (Center for Open Science, Charlottesville, VA, USA, DOI 10.17605/OSF.IO/VTMPW). All scripts for this analysis can be found on Github at https://github.com/niblunc/twin_HCP_paper.

Results

Sample Characteristics. Participant data including age, gender, race/ethnicity, BMI and BMI discordancy, and zygosity can be found in **Table 1**. The BMI-discordant twins ($n_{pairs} = 47$) had a difference > 3.40 kg/m^2, and BMI-similar twins ($n_{pairs} = 47$) had a difference ≤ 1.69 kg/m^2. The distribution of BMI in the three samples can be seen in **Figure 2.**

Connectivity in Body Mass Discordant Twins. Body mass discordant twins (n_{pairs}= 47) had a mean BMI discordancy of 6.7 ± 3.1 kg/m^2, representing a difference greater than one BMI category (NIH, 2017). A within-pair comparison confirmed significant difference in BMI ($T = 7.4$, $p < 0.0001$) between higher BMI and lower BMI twins. Network hierarchy, represented by the brackets in the upper portion of the image, and partial (below the diagonal) and full correlations (above the diagonal) of the 25-network parcellation for the BMI-discordant sample can be seen in **Figure 3A**. Between network connectivity results, controlled for heritability, are summarized in **Table 2.**

When comparing the higher BMI twin to their lower BMI counterpart (higher BMI > lower BMI), we observed significantly stronger connectivity between the occipital pole (IC 9) and a network (IC 2) including the medial orbitofrontal cortex (mOFC), posterior cingulate

cortex/precuneus, temporoparietal junction, and hippocampus, putatively representing the default mode network (DMN; T = 4.30; p_{FWE} = 0.004; Table 2; **Figure 4A**). Stronger connectivity was also observed between the cerebellar right crus I (IC 16) and a network containing the anterior cingulate, insula, central operculum, and precentral gyrus (IC 7; T = 3.64; p_{FWE} = 0.037; Table 2; Figure 4B), and between a network inclusive of the dorsolateral prefrontal cortex (dlPFC) and ventrolateral prefrontal cortex (vlPFC; IC 10) and left crus II of the cerebellum (IC 22; T = 4.57; p_{FWE} = 0.001 Table 2; Figure 4C).

When comparing connectivity of the lower BMI twin relative to the higher BMI twin (lower BMI > higher BMI), significantly stronger connectivity was found between the occipital pole (IC 9) and a network containing the occipital pole (IC 3), intracalcarine cortex, and lingual gyrus (T = 4.04; pFWE = 0.003; Table 2; **Figure 5A**). Stronger connectivity was also found between the occipital pole (IC 9) network and the network inclusive of the insula, anterior cingulate, central operculum, and precentral gyrus networks (IC 7; T = 4.19; pFWE = 0.005; Table 2; Figure 5B). Additionally, stronger connectivity was seen between the dlPFC/vlPFC network (IC 10) and a network including the dorsal and ventral striatum and insula (IC 25; T = 3.70; pFWE = 0.035; Table 2; Figure 5C).

Unique connectivity in Unrelated, Body Mass Discordant Pairs. Network hierarchy and full and partial correlations of the 25-network parcellation for the unrelated, BMI-discordant pairs can be seen in **Figure 3B**. The mean BMI difference between the unrelated, BMI-discordant sample was also 6.7 $\pm$ 3.1 kg/m^2, only 0.12 kg/m^2 different relative to BMI-discordant twin sample (T = 0.06, p = 0.95). Among the higher vs. lower BMI individuals, stronger connectivity was identified between a network identified as the default mode network (IC 2) and a network including the insula, central operculum, precentral gyrus, and anterior cingulate (IC 7; T = 4.71, p = 0.002; Table 2). Stronger connectivity was also observed between a network including the lateral occipital cortex (IC 4) and the lingual gyrus and occipital cortex (IC 12; T = 4.62; p_{FWE} = 0.003). Stronger connectivity was not observed in the lower BMI individuals relative to their higher BMI counterparts in the unrelated pairs.

Unique connectivity in Body Mass Similar Twins. The mean body mass discordance in the BMI-similar twin pairs (n_{pairs} = 47) was 0.7 $\pm$ 0.5 kg/m^2. Network hierarchy and full and partial correlations of the 25-network parcellation can be seen in **Figure 3C**. Connectivity identified in the BMI-similar twin sample was not equivalent with connectivity observed in the BMI-discordant twins, controlling for heritability, there was no significant connectivity observed in either contrast.

100-Network ICA Parcellation. To probe whether connectivity patterns observed in the BMI-discordant twin sample were driven by smaller parcels of networks, we completed the same functional connectivity analyses (including heritability weighting) using the 100-network ICA parcellation in the BMI-discordant twin sample. While significant connectivity was observed in comparing higher BMI > lower BMI twins and lower BMI > higher BMI twins (**Supplement Table 1**), none of the connected networks using the 100 network parcellation reflected similar connectivity patterns seen in the larger networks stemming from the 25-network ICA parcellation.

Secondary Analyses: Behavioral and Physiological Correlates and Differences as a Function of Zygosity. Post-hoc examination of behavioral and physiological characteristics between the two body mass discordant samples revealed no significant interaction of BMI and twin-status on the following: Flanker task scores (T = 0.51, p = 0.61), area under the curve for the $2,000 delay discounting task (T = -0.49, p = 0.62), area under the curve for the $40,000 delay discounting task (T = 0.35, p = 0.73), taste sensitivity task (T = 0.59, p = 0.56), systolic blood pressure (T = 0.56, p = 0.58), diastolic blood pressure (T = 0.76, p = 0.45), and hemoglobin A1c (T = 0.06, p =

0.95), collectively indicating no behavioral or physiological differences between the two body mass discordant samples. Additionally, there were no between group or within pair differences in measures of mood and substance use disorders between the BMI-discordant samples (*p*'s < 0.05). Visual representation of results can be seen in **Supplemental Figure 1**.

Discussion

Leveraging samples of body mass discordant twins, unrelated body mass discordant individuals, and body mass similar twins we sought to determine whether resting state network connectivity was impacted relative differences in BMI. Across the BMI discordant samples, we show that connectivity of networks inclusive of regions previously implicated in encoding gustatory processing (insula/parietal operculum), a network including the primary visual cortex, and the default mode network (DMN) are particularly sensitive to differences in BMI. In both BMI discordant samples, higher BMI individuals show stronger connectivity between default mode network with other networks, specifically the occipital pole (twin sample), and the network inclusive of gustatory processing regions (unrelated sample). Although the between network connectivity stemming from the DMN is different between the two samples, both are in line with previous investigations that indicate elevated BMI is associated with aberrant gustatory and visual processing (Small et al., 2001; Stice et al., 2008; Stoeckel et al., 2008) and with increased connectivity within the DMN (Tregellas et al., 2011). Further, results from BMI discordant samples were not evident in BMI-similar twins, providing support that connectivity results are a function of BMI. Beyond the aforementioned three networks that appear to be consistently sensitive to differences in weight, below we discuss broader implications of the specific BMI dependent between network results.

We observed that the lower BMI twins showed stronger connectivity between a network centered in the dlPFC and a network comprising the striatum/thalamus relative to their higher BMI twins. The predominate regions in these networks are present in mesocorticolimbic dopaminergic circuitry, specifically the mesolimbic (striatum/thalamus) and the mesocortical (dlPFC) dopaminergic pathways (Le Moal and Simon, 1991). Cortical-striatal connectivity is thought to integrate behavioral motivation with decision-making and executive control (Di Martino et al., 2008). Altered cortical-striatal connectivity and decreased dlPFC connectivity has been observed in obesity (García-García et al., 2013; Kullmann et al., 2013, 2012; Moreno-Lopez et al., 2016; Nummenmaa et al., 2012). Here, increased connectivity between these regions confers more efficient communication, indicating lower BMI individuals may be more responsive to changes in reward valuation and present with increased cognitive control during decision-making (Rangel and Hare, 2010), possibly specific to decisions about food intake. This interpretation posits that lighter individuals may possess firmer appetite regulation when presented with highly palatable, energy-dense foods. Previous works supports, the current findings and reinforce the hypothesis that cortical-striatal-thalamic network connectivity is involved with weight regulation through mechanisms where stronger connectivity contributes to better regulation of hedonically motivated food-related behaviors.

Higher BMI twins showed increased connectivity between a network including the insula, central operculum, anterior cingulate, and precentral gyrus with the right crus I of the cerebellum. Regions included in the insular network are consistently implicated in encoding gustatory processing (Veldhuizen et al., 2011), where the right crus I is involved in encoding motor control and working memory (Habas et al., 2009; Stoodley et al., 2012). Positron emission tomography in healthy-weight men demonstrated stronger cerebral blood flow in both the insula and cerebellum when fasted for 36 hours versus a postprandial state (when fed) (Tataranni et al., 1999), indicating the strength of his dynamic connectivity may be associated with caloric deprivation. In support, functional connectivity between insular and cerebellar networks in healthy weight individuals was also elevated following an overnight fast (Wright et al., 2016). Moreover, insular-cerebellar connectivity is seen in healthy individuals during

hypoglycemia (Bolo et al., 2015), a physiologic characteristic of being fasted for extended time periods. Taken together, these data provide strong evidence that stronger insula and cerebellar connectivity is reflective of caloric deprivation/hunger signaling. Interestingly, in obese individuals, increased insula and cerebellar BOLD response were seen following gastric distension by balloon, mimicking fullness without a caloric load (Tomasi et al., 2009). This supports the notion that higher BMI individuals show an insular-cerebellar response that is thought to encode aspects of being calorically deprived in a time their stomach is 'full'. This BMI dependent incongruent valence of insula and cerebellar connectivity could act to perpetuate food intake in a postprandial state, commonly referred to as eating in the absence of hunger. In support, behavioral reports demonstrate that obesity is associated with increased appetite and decreased satiation (Cabanac and Duclaux, 1970; Schachter, 1968). In sum, these data signify that, unlike being a healthy weight, higher BMI is associated with a stronger insula-cerebellar connection that is unresponsive to fullness, theoretically, contributing to increased postprandial food intake.

Elevated BMI was also related to stronger connectivity between the primary visual cortex and the DMN, which the latter is reflective of internal mental awareness and is diminished during goal-directed tasks (Buckner et al., 2008). At rest, functional connectivity within the DMN is positively correlated with BMI (Tregellas et al., 2011), and obesity is associated with increased connectivity within the salience network, which comprises the visual cortex and superior parietal lobule (including the precuneus/PCC) (García-García et al., 2013). Moreover, evoked studies utilizing food stimuli (pictures of foods, cue-elicited anticipation of food receipt) consistently demonstrate that elevated weight is associated increased BOLD response in these regions that encode visual and attentional processing. This pattern of higher propensity towards strong visual response with elevated weight is hypothesized to play a key role forming eating habits (Gilbert and Burger, 2016).

The general approach used here, i.e., comparison the higher BMI versus lower BMI, does not directly align with comparisons of 'standard' weight status groupings, i.e., obese versus healthy weight (NIH, 2017). While our study is cross-sectional, the present approach is more relevant to longitudinal and experimental designs. Prospective designs typically use within-subject continuous BMI change as a sensitive test for weight change, for example a shift from a 'healthy' BMI of 24.5 to an 'overweight' BMI of 25.3 is clinically insignificant. In the present sample, there are relatively broad distributions of BMI in both the 'higher BMI' and 'lower BMI' groups. Results from these analyses cannot provide valid information regarding the relationship between functional connectivity and absolute BMI. Due to the analysis used, one cannot infer that any given BMI is related to a specific connectivity pattern based on solely this data, one can only interpret the results in terms of relative higher and lower body mass. In support of the present approach, it has been suggested that absolute BMI is not the best standard of health, as it does not always align with health and mortality outcomes (Nuttall, 2015). Moreover, when individuals are at an elevated weight, a 5% weight loss is physiologically beneficial (Douketis et al., 2005). The present design dovetails with this clinically relevant 'relative weight difference' approach, making results more applicable to prospective and intervention studies. Though, the approach does require consideration of the magnitude of BMI difference within pairs. Here, BMI-discordant twin pairs had an average BMI difference of 6.7 kg/m^2. Although this difference greater than a full BMI category, within some pairs, the heavy and lighter individuals were in the same BMI category, or both obese and overweight. As such, we were not surprised that the patterns of connectivity observed in this study differ somewhat from previous analyses based on BMI categories (García-García et al., 2013; Kullmann et al., 2012; Park et al., 2016; Wijngaarden et al., 2015).

No equivalent connectivity was observed between BMI-discordant twins and the unrelated, BMI-discordant pairs. Twins inherently have shared genetics, likely have a similar food environment during youth (Barsh et al., 2000; Farooqi and O'rahilly, 2000), demonstrate less

between-subject variability in common fMRI confounds, i.e., head motion (Hodgson et al., 2016), and show similar resting state network connectivity (Fu et al., 2015). By largely controlling for these possible confounds (Falconer and Mackay, 1996), results from the BMI-discordant twin sample may provide a robust test for BMI-dependent differences in connectivity. However, this approach cannot completely account for every aspect of heritability and/or shared early life environment. The remaining possible confounders could be represented in the lack of consistent results between two BMI-discordant samples. This possibility demonstrates a decision point in study design, specifically, the comparing relative importance of internal sensitivity and/or high methodological study control, relative to generalizability of results. Here, the twin sample approach is more highly controlled, and thus the results are likely to be closer to true effect of body mass on functional connectivity. However, even if that notion is correct, the 'true' results are of limited utility as they only generalize to twins, where a case can be made that the results from the unrelated sample are more meaningful as they generalize to a larger population. Ultimately, replication of findings in independent samples, across multiple studies, utilizing different data acquisition techniques will serve to establish both validity and generalizability of the results.

We did not find significant within pair differences between BMI-discordant twins or unrelated BMI-discordant pairs in behavioral (executive functioning, impulsivity, and taste sensitivity) and physiological measures (hemoglobin A1c and blood pressure) that are thought to be associated with weight. Eligibility criteria excluded individuals with weight-related diseases, e.g. individuals with high blood pressure and/or diabetes, thereby reducing the variability in these behavioral and physiological measures and thus the ability to detect BMI-related differences between higher BMI and lower BMI twins. Additionally, the differences in functional connectivity observed may not manifest behaviorally in the measures included in the present sample, specifically given these generalized tasks, i.e., not food specific. In support, previous weight discordant twin research, heavier twins reported stronger preference for fat and a greater tendency to overeat, but no difference on non-food related psychological measures (Rissanen et al., 2002). This suggests that testing food/eating behaviors specific measures may better identify differences as a function of weight status, but generalized assessments may have lower sensitivity when assessing BMI-related differences.

In the primary analysis, we assessed between network connectivity within the 25 networks identified by ICA parcellation, though it reasonable to hypothesize that additional differences between weight discordant twins may emerge at a higher dimensionality, as it potentially parses apart large networks into smaller sub-regions. The exploratory connectivity analysis using a 100-network parcellation attempted to address this limitation, however this did not elicit identifiable 'sub'-networks for more specific interpretation. These data indicate that broader networks that incorporate more regions, may provide more meaningful information relating to our hypotheses. However, this approach did lend itself to significant connectivity patterns of networks that are anatomically located next to one another, i.e., (IC 9 with IC 3; IC 4 with IC 12). As the regions in each network are too similar in function for meaningful interpretation, for the brevity of this discussion these patterns were not discussed. The present study is restricted by its cross-sectional design, limiting inferences regarding the temporal precedence of the relations between functional connectivity and BMI. We are unable to determine a causal nature of the observed relationships between weight and differential functional connectivity and can only state that these differences in connectivity may play a role associated with weight regulation.

In sum, this investigation examined functional connectivity between weight discordant twins and unrelated samples. We observed that, across all of the samples tested, a network compromised of gustatory processing regions, a visual processing network, and the default mode network all appear to be highly sensitivity to weight status. Further, reduced weight is associated with greater integration of regions that encode reward learning and executive control which underpin hedonically motived behaviors. This, theoretically, may contribute to better

behavioral control when lighter individuals are faced with highly palatable foods. Lastly, higher weight is associated with functional connectivity pattern that has consistently been reflective of caloric deprivation/hunger. Here, we demonstrate that unique, distinct connectivity patterns can represent weight variability adding to the mounting evidence that implicates aberrant brain functioning with the accumulation and/or maintenance of elevated weight.

Acknowledgements
The authors would like to thank Dr. Steve Smith for assistance with utilization of Human Connectome Project data and selection of the analytic approach.

Author contributions
JRS completed study preregistration, analyses, and drafted the manuscript. GES assisted in study development, analyses, and revised the manuscript. KSB contributed to study development, analyses, and drafting the manuscript.

Competing financial interests statement
The authors declare no competing financial interests.

Table 1: Participant Characteristics (n=282[a])

	BMI-discordant twins (n=94)	**Unrelated, BMI-discordant pairs** (n=94)	Group Difference *BMI-discordant twins & unrelated pairs*	**BMI-similar twins** (n=94)	Group Difference *BMI-discordant twins & BMI-similar twins*
Age (mean ± SD; years)	29.4 ± 3.5	28.5 ± 3.6	$p = 0.08$	29.3 ± 3.5	$p = 0.71$
Body Mass Index (kg/m^2)	28.1 ± 5.6	28.1 ± 5.7	$p = 0.95$	25.6 ± 4.1	**$p < 0.001$**
BMI Discordancy (kg/m^2)	6.7 ± 3.1	6.7 ± 3.1	$p = 0.98$	0.7 ± 0.5	**$p < 0.001$**
Race (percent)					
Asian/Pacific Islander	0	9 (10%)		7 (7%)	
African American	14 (15%)	21 (22%)	**$p = 0.002$**	10 (11%)	**$p = 0.02$**
Caucasian	78 (83%)	58 (62%)		77 (82%)	
Multiracial	0	3 (3%)		0	
Not Reported	2 (2%)	3 (3%)		0	
Ethnicity (percent)					
Hispanic/Latino	1 (1%)	12 (13%)	**$p = 0.003$**	0	$p = 0.51$
Non-Hispanic/Latino	91 (97%)	82 (87%)		93 (99%)	
Not Reported	2 (2%)	0		1 (1%)	
Zygosity (percent)					
Monozygotic	44 (47%)	N/A	N/A	44 (47%)	$p = 1.0$
Dizygotic	50 (53%)	N/A		50 (53%)	
Gender (percent)					
Male	32 (34%)	32 (34%)	$p = 1.0$	46 (49%)	$p = 0.05$
Female	62 (66%)	62 (66%)		48 (51%)	

[a] Total unique subjects across the three samples included in analyses

* Significant group difference between the BMI-discordant twin sample and the unrelated, BMI-discordant pair sample or BMI-similar twin sample, as determined by t-test (age, BMI, BMI discordancy) or χ^2 test (race, ethnicity, zygosity, gender) ($p < 0.05$)

Table 2: Significant Between Network Connectivity in BMI-discordant Twins (n=94) and Unrelated, BMI-Discordant Pairs (n=94)

BMI-Discordant Twins

Contrast	*IC*	*Network*	*T-value*	p_{FWE}
Higher BMI > Lower BMI	9	Occipital pole	4.30	0.004
	2	Default Mode Network		
	16	Right crus I	3.64	0.037
	7	Insula, central operculum, precentral gyrus, and anterior cingulate		
	10	Dorsolateral prefrontal cortex, ventrolateral prefrontal cortex	4.57	0.001
	22	Left crus II		
Lower BMI > Higher BMI	9	Occipital pole	4.04	0.003
	3	Occipital pole, intracalcarine cortex, and lingual gyrus		
	9	Occipital pole	4.19	0.005
	7	Insula, central operculum, precentral gyrus, and anterior cingulate		
	10	Dorsolateral prefrontal cortex, ventrolateral prefrontal cortex	3.70	0.035
	25	Dorsal striatum, ventral striatum, insula		

Unrelated, BMI-Discordant Pairs

Contrast	*IC*	*Network*	*T-value*	p_{FWE}
Higher BMI > Lower BMI	2	Default Mode Network	4.71	0.002
	7	Insula, parietal operculum, and dorsal anterior cingulate cortex		
	4	Lateral occipital cortex	4.62	0.003
	12	Lingual gyrus, occipital cortex		

Figure 1

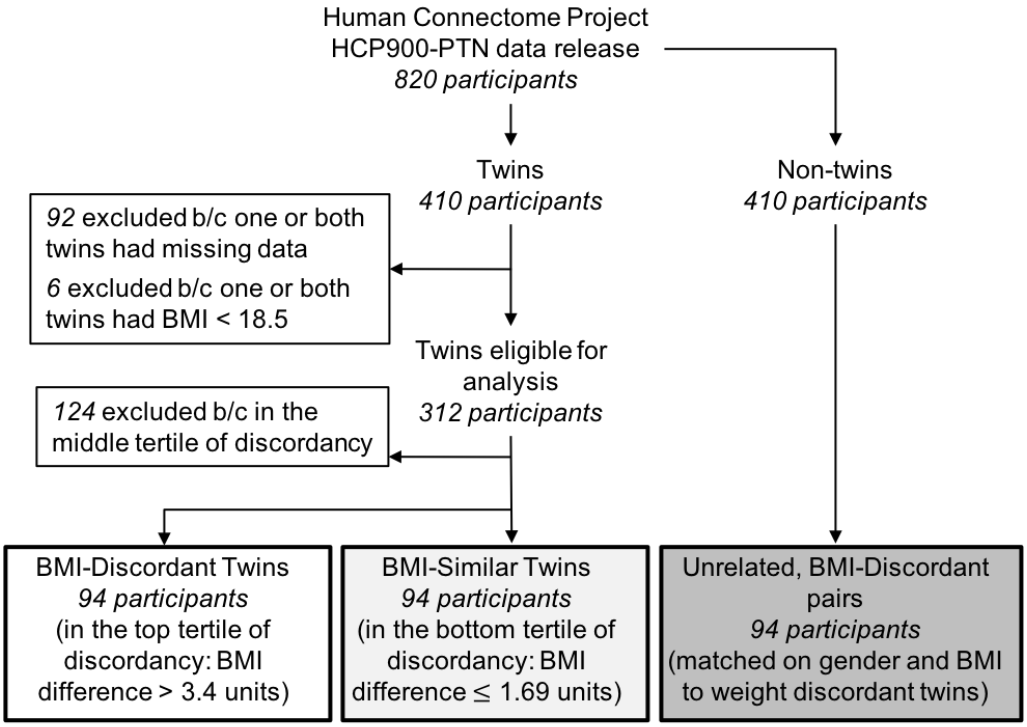

Total n = 282

The selection procedure used to generate the three main samples for the study analyses from the Human Connectome Project HCP900-PTN data release.

Figure 2.

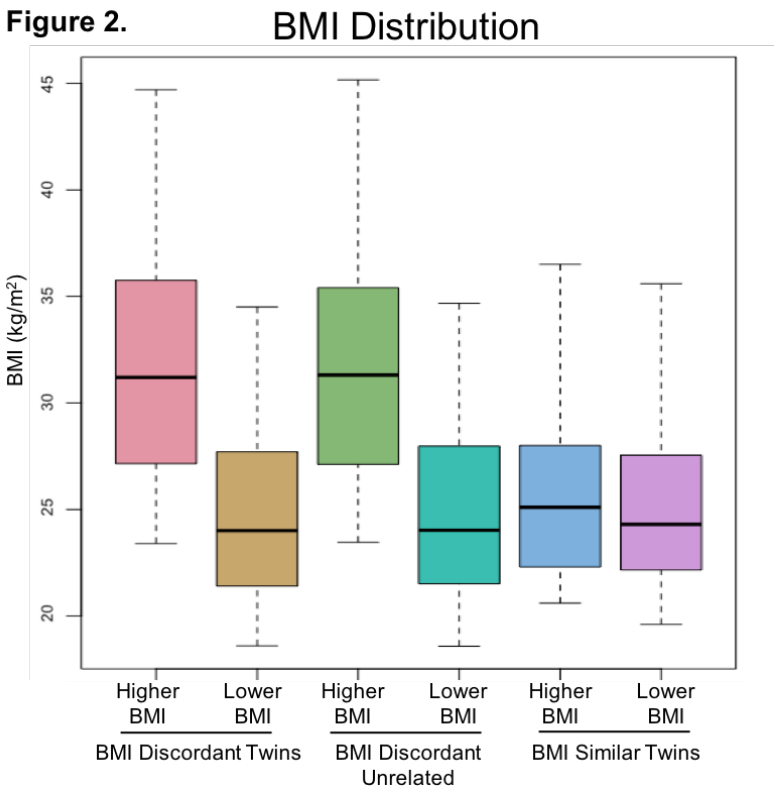

BMI distributions of the higher and lower BMI individuals within the BMI discordant twin group, BMI discordant unrelated pair group, and BMI similar twin group.

Figure 3.

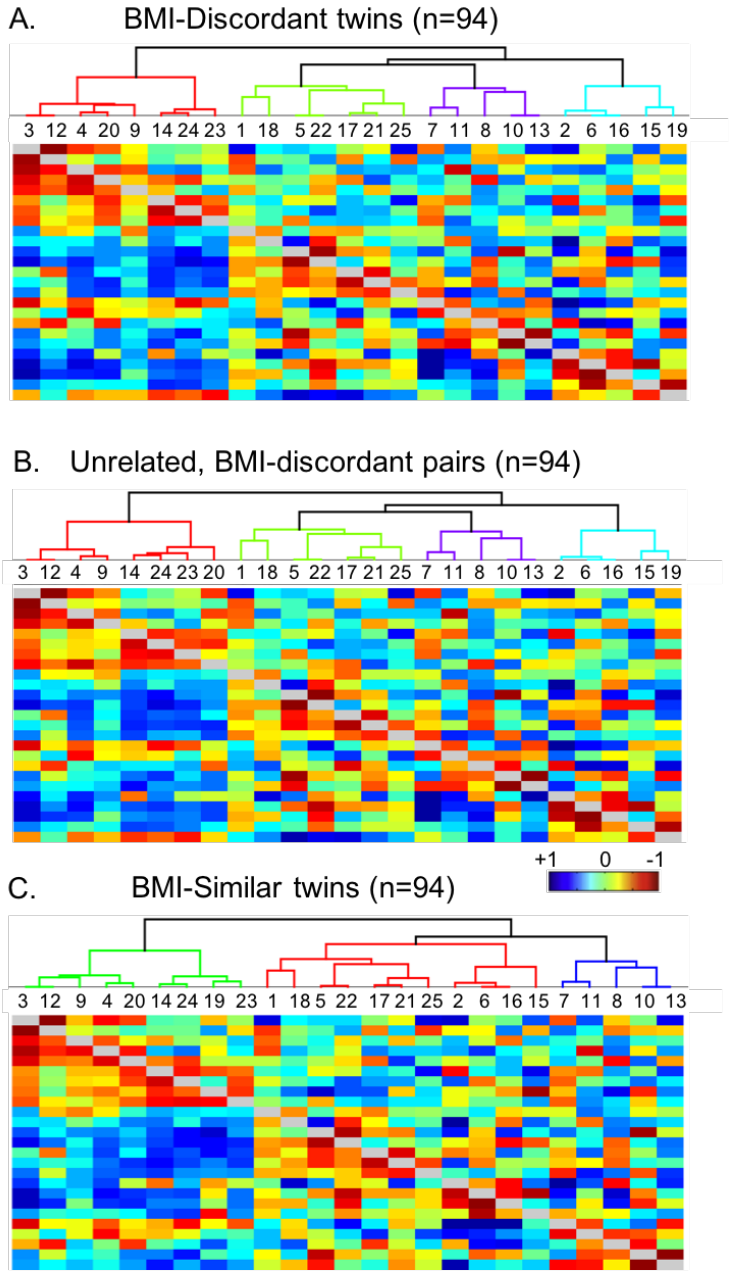

Hierarchy and correlation heatmaps of resting state network connectivity in the three independent samples tested: **A**) BMI-discordant twins; **B**) unrelated, BMI-discordant pairs; **C**) BMI similar twins, for the 25-network parcellation. Each map shows the parcel hierarchy at the top (brackets); independent component (IC) numbers listed in the row below the hierarchy; full correlation values in the upper portion of the heatmap, and partial correlation values in the lower portion of the heatmap.

501
502

Figure 4.

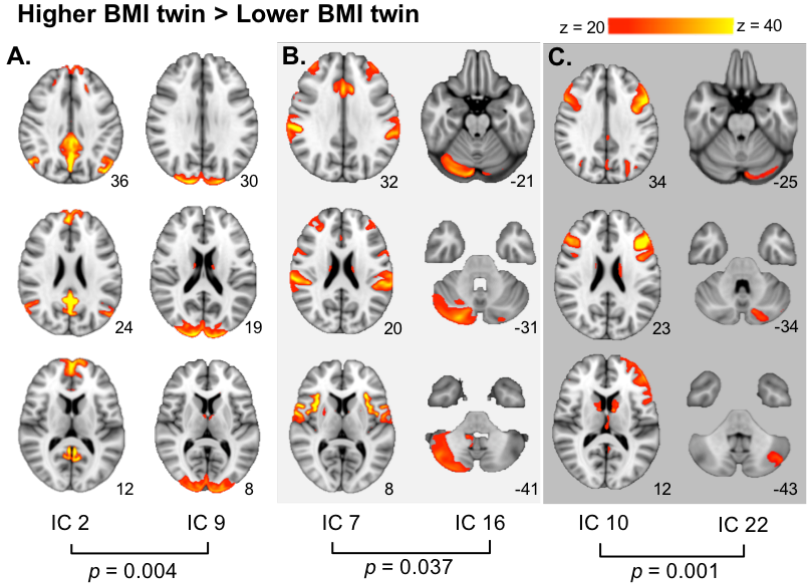

Differential network connectivity in the BMI-discordant twin sample. When contrasting higher BMI > lower BMI, stronger connectivity was seen between: **A.** the default mode network (IC 2) and the occipital pole (IC 9); **B.** the insula, central operculum, precentral gyrus and anterior cingulate (IC 7) and right crus I of the cerebellum (IC 16); **C.** the dorsolateral prefrontal cortex and ventrolateral prefrontal cortex (IC 10) and the left crus II (IC 22). MNI coordinates of each slice on the z-axis are listed below each slice.

Figure 5.

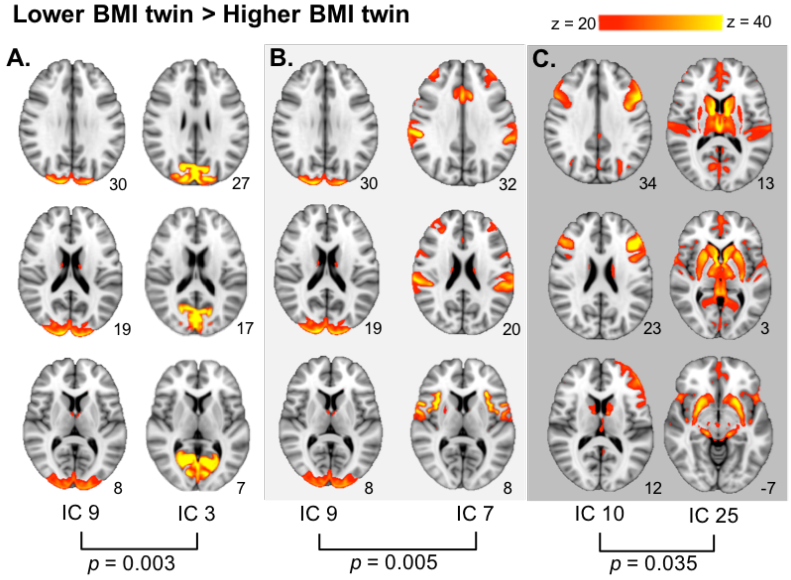

Differential network connectivity in the BMI-discordant twin sample. When contrasting lower BMI > higher BMI, stronger connectivity was found between: **A.** the occipital pole, intracalcarine cortex, and lingual gyrus (IC 3) and the occipital pole (IC 9); **B.** the occipital pole (IC 9) and the insula, central operculum, precentral gyrus and anterior cingulate (IC 7); **C.** the dorsolateral prefrontal cortex and ventrolateral prefrontal cortex (IC 10) and the dorsal striatum, ventral striatum, and insula (IC 25). MNI coordinates of each slice on the z-axis are listed below each slice.

References

Alberti, K.G.M.M., Zimmet, P., Shaw, J., 2005. The metabolic syndrome—a new worldwide definition. Lancet 366, 1059–1062.

Barsh, G.S., Farooqi, I.S., O'rahilly, S., 2000. Genetics of body-weight regulation. Nature 404, 644–651.

Berthoud, H., 2006. Homeostatic and non-homeostatic pathways involved in the control of food intake and energy balance. Obesity 14.

Blackburn, G., 1995. Effect of degree of weight loss on health benefits. Obesity 3.

Bolo, N.R., Musen, G., Simonson, D.C., Nickerson, L.D., Flores, V.L., Siracusa, T., Hager, B., Lyoo, I.K., Renshaw, P.F., Jacobson, A.M., 2015. Functional connectivity of insula, basal ganglia, and prefrontal executive control networks during hypoglycemia in type 1 diabetes. J. Neurosci. 35, 11012–11023.

Buckner, R.L., Andrews-Hanna, J.R., Schacter, D.L., 2008. The brain's default network. Ann. N. Y. Acad. Sci. 1124, 1–38.

Cabanac, M., Duclaux, R., 1970. Obesity: Absence of satiety aversion to sucrose. Science (80-.). 168, 496–497.

Calle, E.E., Kaaks, R., 2004. Overweight, obesity and cancer: epidemiological evidence and proposed mechanisms. Nat. Rev. Cancer 4, 579.

Coldwell, S.E., Mennella, J.A., Duffy, V.B., Pelchat, M.L., Griffith, J.W., Smutzer, G., Cowart, B.J., Breslin, P.A.S., Bartoshuk, L.M., Hastings, L., 2013. Gustation assessment using the NIH Toolbox. Neurology 80, S20--S24.

Collaborators, G., 2017. Health Effects of Overweight and Obesity in 195 Countries over 25 Years. N. Engl. J. Med.

Di Martino, A., Scheres, A., Margulies, D.S., Kelly, A.M.C., Uddin, L.Q., Shehzad, Z., Biswal, B., Walters, J.R., Castellanos, F.X., Milham, M.P., 2008. Functional connectivity of human striatum: a resting state FMRI study. Cereb. cortex 18, 2735–2747.

Dombrowski, S.U., Knittle, K., Avenell, A., Araujo-Soares, V., Sniehotta, F.F., 2014. Long term maintenance of weight loss with non-surgical interventions in obese adults: systematic review and meta-analyses of randomised controlled trials. Bmj 348, g2646.

Doornweerd, S., van Duinkerken, E., de Geus, E.J., Arbab-Zadeh, P., Veltman, D.J., IJzerman, R.G., 2017. Overweight is associated with lower resting state functional connectivity in females after eliminating genetic effects: A twin study. Hum. Brain Mapp. 38, 5069–5081.

Douketis, J.D., Macie, C., Thabane, L., Williamson, D.F., 2005. Systematic review of long-term weight loss studies in obese adults: clinical significance and applicability to clinical practice. Int. J. Obes. 29, 1153.

Eklund, A., Nichols, T.E., Knutsson, H., 2016. Cluster failure: why fMRI inferences for spatial extent have inflated false-positive rates. Proc. Natl. Acad. Sci. 201602413.

Falconer, D.S., Mackay, T.F.C., 1996. Introduction to quantitative genetics. Longmans Green, Harlow, Essex, UK. Introd. to Quant. Genet. 4th ed. Longmans Green, Harlow, Essex, UK.

Farooqi, I.S., O'rahilly, S., 2000. Recent advances in the genetics of severe childhood obesity. Arch. Dis. Child. 83, 31–34.

Filippini, N., MacIntosh, B.J., Hough, M.G., Goodwin, G.M., Frisoni, G.B., Smith, S.M., Matthews, P.M., Beckmann, C.F., Mackay, C.E., 2009. Distinct patterns of brain activity in young carriers of the APOE-epsilon4 allele. Proc. Natl. Acad. Sci. U. S. A. 106, 7209–7214. doi:10.1073/pnas.0811879106

Flegal, K.M., Carroll, M.D., Kit, B.K., Ogden, C.L., 2012. Prevalence of Obesity and Trends in the Distribution of Body Mass Index Among US Adults, 1999-2010. Jama-Journal Am. Med. Assoc. 307, 491–497. doi:10.1001/jama.2012.39

Fu, Y., Ma, Z., Hamilton, C., Liang, Z., Hou, X., Ma, X., Hu, X., He, Q., Deng, W., Wang, Y., 2015. Genetic influences on resting-state functional networks: A twin study. Hum. Brain

Mapp. 36, 3959–3972.
García-García, I., Jurado, M.Á., Garolera, M., Segura, B., Sala-Llonch, R., Marqués-Iturria, I., Pueyo, R., Sender-Palacios, M.J., Vernet-Vernet, M., Narberhaus, A., 2013. Alterations of the salience network in obesity: a resting-state fMRI study. Hum. Brain Mapp. 34, 2786–2797.
Geha, P., Cecchi, G., Todd Constable, R., Abdallah, C., Small, D.M., 2016. Reorganization of brain connectivity in obesity. Hum. Brain Mapp.
Gilbert, J.R., Burger, K.S., 2016. Neuroadaptive processes associated with palatable food intake: present data and future directions. Curr. Opin. Behav. Sci. 9, 91–96.
Glahn, D.C., Winkler, A.M., Kochunov, P., Almasy, L., Duggirala, R., Carless, M.A., Curran, J.C., Olvera, R.L., Laird, A.R., Smith, S.M., 2010. Genetic control over the resting brain. Proc. Natl. Acad. Sci. 107, 1223–1228.
Glasser, M.F., Coalson, T.S., Robinson, E.C., Hacker, C.D., Harwell, J., Yacoub, E., Ugurbil, K., Andersson, J., Beckmann, C.F., Jenkinson, M., Smith, S.M., Van Essen, D.C., 2016. A multi-modal parcellation of human cerebral cortex. Nature 536, 171–178. doi:10.1038/nature18933
Glasser, M.F., Sotiropoulos, S.N., Wilson, J.A., Coalson, T.S., Fischl, B., Andersson, J.L., Xu, J., Jbabdi, S., Webster, M., Polimeni, J.R., 2013. The minimal preprocessing pipelines for the Human Connectome Project. Neuroimage 80, 105–124.
Green, L., Fristoe, N., Myerson, J., 1994. Temporal discounting and preference reversals in choice between delayed outcomes. Psychon. Bull. {&} Rev. 1, 383–389.
Grinker, J., Hirsch, J., Smith, D. V, 1972. Taste sensitivity and susceptibility to external influence in obese and normal weight subjects. J. Pers. Soc. Psychol. 22, 320.
Habas, C., Kamdar, N., Nguyen, D., Prater, K., Beckmann, C.F., Menon, V., Greicius, M.D., 2009. Distinct cerebellar contributions to intrinsic connectivity networks. J. Neurosci. 29, 8586–8594.
Hodgson, K., Poldrack, R.A., Curran, J.E., Knowles, E.E., Mathias, S., Göring, H.H.H., Yao, N., Olvera, R.L., Fox, P.T., Almasy, L., 2016. Shared genetic factors influence head motion during mri and body mass index. Cereb. Cortex 1–8.
Hubert, H.B., Feinleib, M., McNamara, P.M., Castelli, W.P., 1983. Obesity as an independent risk factor for cardiovascular disease: a 26-year follow-up of participants in the Framingham Heart Study. Circulation 67, 968–977.
Jensen, M.D., Ryan, D.H., Apovian, C.M., Ard, J.D., Comuzzie, A.G., Donato, K.A., Hu, F.B., Hubbard, V.S., Jakicic, J.M., Kushner, R.F., 2013. 2013 AHA/ACC/TOS Guideline for the Management of Overweight and Obesity in Adults. Circulation 01–cir.
Kukull, W.A., Ganguli, M., 2012. Generalizability The trees, the forest, and the low-hanging fruit. Neurology 78, 1886–1891.
Kullmann, S., Heni, M., Veit, R., Ketterer, C., Schick, F., Häring, H.-U.H.H.-U., Fritsche, A., Preissl, H., 2012. The obese brain: association of body mass index and insulin sensitivity with resting state network functional connectivity. Hum. Brain Mapp. 33, 1052–1061. doi:10.1002/hbm.21268
Kullmann, S., Pape, A.-A., Heni, M., Ketterer, C., Schick, F., Häring, H.-U., Fritsche, A., Preissl, H., Veit, R., 2013. Functional network connectivity underlying food processing: disturbed salience and visual processing in overweight and obese adults. Cereb. Cortex 23, 1247–1256. doi:10.1093/cercor/bhs124
Lavagnino, L., Arnone, D., Cao, B., Soares, J.C., Selvaraj, S., 2016. Inhibitory control in obesity and binge eating disorder: A systematic review and meta-analysis of neurocognitive and neuroimaging studies. Neurosci. Biobehav. Rev. 68, 714–726.
Le Moal, M., Simon, Herv., 1991. Mesocorticolimbic dopaminergic network: functional and regulatory roles. Physiol. Rev. 71, 155–234.
Lips, M.A., Wijngaarden, M.A., van der Grond, J., van Buchem, M.A., de Groot, G.H.,

608 Rombouts, S.A., Pijl, H., Veer, I.M., 2014. Resting-state functional connectivity of brain
609 regions involved in cognitive control, motivation, and reward is enhanced in obese females.
610 Am J Clin Nutr 100, 524–531. doi:10.3945/ajcn.113.080671
611 Loveman, E., Frampton, G.K., Shepherd, J., Picot, J., Cooper, K., Bryant, J., Welch, K., Clegg,
612 A., 2011. The clinical effectiveness and cost-effectiveness of long-term weight
613 management schemes for adults: a systematic review.
614 Masters, R.K., Reither, E.N., Powers, D.A., Yang, Y.C., Burger, A.E., Link, B.G., 2013. The
615 impact of obesity on US mortality levels: the importance of age and cohort factors in
616 population estimates. Am. J. Public Health 103, 1895–1901.
617 Moreno-Lopez, L., Contreras-Rodriguez, O., Soriano-Mas, C., Stamatakis, E.A., Verdejo-
618 Garcia, A., 2016. Disrupted functional connectivity in adolescent obesity. NeuroImage Clin.
619 12, 262–268.
620 Morton, G.J., Cummings, D.E., Baskin, D.G., Barsh, G.S., Schwartz, M.W., 2006. Central
621 nervous system control of food intake and body weight. Nature 443, 289–295.
622 Murphy, K., Birn, R.M., Handwerker, D.A., Jones, T.B., Bandettini, P.A., 2009. The impact of
623 global signal regression on resting state correlations: are anti-correlated networks
624 introduced? Neuroimage 44, 893–905.
625 Nederkoorn, C., Braet, C., Van Eijs, Y., Tanghe, A., Jansen, A., 2006. Why obese children
626 cannot resist food: the role of impulsivity. Eat. Behav. 7, 315–322.
627 Nederkoorn, C., Jansen, E., Mulkens, S., Jansen, A., 2007. Impulsivity predicts treatment
628 outcome in obese children. Behav. Res. Ther. 45, 1071–1075.
629 NIH, 2017. Body Mass Index Table [WWW Document]. Natl. Hear. Lung, Blood Inst.
630 Nummenmaa, L., Hirvonen, J., Hannukainen, J.C., Immonen, H., Lindroos, M.M., Salminen, P.,
631 Nuutila, P., 2012. Dorsal Striatum and Its Limbic Connectivity Mediate Abnormal
632 Anticipatory Reward Processing in Obesity. PLoS One 7.
633 doi:10.1371/journal.pone.0031089
634 Nuttall, F.Q., 2015. Body mass index: obesity, BMI, and health: a critical review. Nutr. Today 50,
635 117.
636 Park, B.-Y., Seo, J., Park, H., 2016. Functional brain networks associated with eating behaviors
637 in obesity. Sci. Rep. 6, 23891. doi:10.1038/srep23891
638 Poldrack, R.A., Mumford, J.A., Nichols, T.E., 2011. Handbook of functional MRI data analysis.
639 Cambridge University Press.
640 Rangel, A., Hare, T., 2010. Neural computations associated with goal-directed choice. Curr.
641 Opin. Neurobiol. 20, 262–270.
642 Ray, K.L., McKay, D.R., Fox, P.M., Riedel, M.C., Uecker, A.M., Beckmann, C.F., Smith, S.M.,
643 Fox, P.T., Laird, A.R., 2013. ICA model order selection of task co-activation networks.
644 Front. Neurosci. 7.
645 Rissanen, A., Hakala, P., Lissner, L., Mattlar, C.E., Koskenvuo, M., Ronnemaa, T., Rönnemaa,
646 T., 2002. Acquired preference especially for dietary fat and obesity: a study of weight-
647 discordant monozygotic twin pairs. Int. J. Obes. 26, 973. doi:10.1038/sj.ijo.0802014
648 Robinson, E.C., Jbabdi, S., Glasser, M.F., Andersson, J., Burgess, G.C., Harms, M.P., Smith,
649 S.M., Van Essen, D.C., Jenkinson, M., 2014. MSM: A new flexible framework for
650 Multimodal Surface Matching. Neuroimage 100, 414–426.
651 doi:10.1016/j.neuroimage.2014.05.069
652 Salimi-Khorshidi, G., Douaud, G., Beckmann, C.F., Glasser, M.F., Griffanti, L., Smith, S.M.,
653 2014. Automatic denoising of functional MRI data: combining independent component
654 analysis and hierarchical fusion of classifiers. Neuroimage 90, 449–468.
655 Schachter, S., 1968. Obesity and eating. Science (80-.).
656 Small, D.M., Zatorre, R.J., Dagher, A., Evans, A.C., Jones-Gotman, M., 2001. Changes in brain
657 activity related to eating chocolate from pleasure to aversion. Brain 124, 1720–1733.
658 Smith, S.M., Beckmann, C.F., Andersson, J., Auerbach, E.J., Bijsterbosch, J., Douaud, G., Duff,

659 E., Feinberg, D.A., Griffanti, L., Harms, M.P., 2013. Resting-state fMRI in the human
660 connectome project. Neuroimage 80, 144–168.
661 Smith, S.M., Hyvärinen, A., Varoquaux, G., Miller, K.L., Beckmann, C.F., 2014. Group-PCA for
662 very large fMRI datasets. Neuroimage 101, 738–749.
663 Stice, E., Spoor, S., Bohon, C., Veldhuizen, M.G., Small, D.M., 2008. Relation of Reward From
664 Food Intake and Anticipated Food Intake to Obesity: A Functional Magnetic Resonance
665 Imaging Study. J. Abnorm. Psychol. 117, 924–935. doi:10.1037/a0013600
666 Stoeckel, L.E., Weller, R.E., Cook III, E.W., Twieg, D.B., Knowlton, R.C., Cox, J.E., 2008.
667 Widespread reward-system activation in obese women in response to pictures of high-
668 calorie foods. Neuroimage 41, 636–647. doi:10.1016/j.neuroimage.2008.02.031
669 Stoodley, C.J., Valera, E.M., Schmahmann, J.D., 2012. Functional topography of the cerebellum
670 for motor and cognitive tasks: an fMRI study. Neuroimage 59, 1560–1570.
671 Tataranni, P.A., Gautier, J.-F., Chen, K., Uecker, A., Bandy, D., Salbe, A.D., Pratley, R.E.,
672 Lawson, M., Reiman, E.M., Ravussin, E., 1999. Neuroanatomical correlates of hunger and
673 satiation in humans using positron emission tomography. Proc. Natl. Acad. Sci. 96, 4569–
674 4574.
675 Tomasi, D., Wang, G.-J., Wang, R., Backus, W., Geliebter, A., Telang, F., Jayne, M.C., Wong,
676 C., Fowler, J.S., Volkow, N.D., 2009. Association of body mass and brain activation during
677 gastric distention: implications for obesity. PLoS One 4, e6847.
678 Tregellas, J.R., Wylie, K.P., Rojas, D.C., Tanabe, J., Martin, J., Kronberg, E., Cordes, D.,
679 Cornier, M.-A., 2011. Altered default network activity in obesity. Obesity (Silver Spring). 19,
680 2316–2321. doi:10.1038/oby.2011.119
681 Van Den Heuvel, M.P., Pol, H.E.H., 2010. Exploring the brain network: a review on resting-state
682 fMRI functional connectivity. Eur. Neuropsychopharmacol. 20, 519–534.
683 Van Essen, D.C., Ugurbil, K., Auerbach, E., Barch, D., Behrens, T.E.J., Bucholz, R., Chang, A.,
684 Chen, L., Corbetta, M., Curtiss, S.W., 2012. The Human Connectome Project: a data
685 acquisition perspective. Neuroimage 62, 2222–2231.
686 Veldhuizen, M.G., Albrecht, J., Zelano, C., Boesveldt, S., Breslin, P., Lundström, J.N., 2011.
687 Identification of human gustatory cortex by activation likelihood estimation. Hum. Brain
688 Mapp. 32, 2256–2266.
689 Weintraub, S., Dikmen, S.S., Heaton, R.K., Tulsky, D.S., Zelazo, P.D., Bauer, P.J., Carlozzi,
690 N.E., Slotkin, J., Blitz, D., Wallner-Allen, K., 2013. Cognition assessment using the NIH
691 Toolbox. Neurology 80, S54--S64.
692 Wijngaarden, M.A., Veer, I.M., Rombouts, S., van Buchem, M.A., van Dijk, K.W., Pijl, H., van
693 der Grond, J., 2015. Obesity is marked by distinct functional connectivity in brain networks
694 involved in food reward and salience. Behav. Brain Res. 287, 127–134.
695 Winkler, A.M., Ridgway, G.R., Webster, M.A., Smith, S.M., Nichols, T.E., 2014. Permutation
696 inference for the general linear model. Neuroimage 92, 381–397.
697 doi:10.1016/j.neuroimage.2014.01.060
698 Woodward, N.D., Cascio, C.J., 2015. Resting-state functional connectivity in psychiatric
699 disorders. JAMA psychiatry 72, 743–744.
700 Wright, H., Li, X., Fallon, N.B., Crookall, R., Giesbrecht, T., Thomas, A., Halford, J.C.G.,
701 Harrold, J., Stancak, A., 2016. Differential effects of hunger and satiety on insular cortex
702 and hypothalamic functional connectivity. Eur. J. Neurosci. 43, 1181–1189.
703 Yang, Z., Zuo, X.-N., McMahon, K.L., Craddock, R.C., Kelly, C., de Zubicaray, G.I., Hickie, I.,
704 Bandettini, P.A., Castellanos, F.X., Milham, M.P., 2016. Genetic and environmental
705 contributions to functional connectivity architecture of the human brain. Cereb. Cortex 26,
706 2341–2352.
707